Available online at www.sciencedirect.com
ScienceDirect
International Journal of Heat and Mass Transfer 50 (2007) 3302–3314
International Journal of HEAT and MASS TRANSFER
www.elsevier.com/locate/ijhmt

Jet impingement heat transfer – Part II: A temporal investigation of heat transfer and local fluid velocities

Tadhg S. O'Donovan *, Darina B. Murray

Department of Mechanical and Manufacturing Engineering, Trinity College Dublin, Ireland

Received 1 August 2006; received in revised form 28 January 2007
Available online 5 April 2007

Abstract

Impinging jets are a means of achieving high heat transfer coefficients both locally and on an area averaged basis. The temporal nature of both the fluid flow and heat transfer has been investigated for Reynolds numbers from 10,000 to 30,000 and non-dimensional surface to jet exit distance, H/D, from 0.5 to 8. At the impingement surface simultaneous acquisition of both local heat flux and local velocity signal has facilitated a comprehensive analysis of the effect that fluid flow has on the heat transfer. Results are presented in the form of surface heat transfer and fluid velocity signal spectra, and coherence and phase difference between the corresponding velocity and heat flux signals. It has been shown that the evolution of vortices with distance from the jet exit has an influence on the magnitude of the heat transfer coefficient in the wall jet.

Keywords: Jet impingement; Heat transfer; Vortices; Spectra; Coherence; Phase

1. Introduction

Impinging air jets are employed in a wide range of applications for enhanced cooling, as detailed in the first part of this two part investigation. The effect of local mean velocities and turbulence intensities on the heat transfer has been outlined in part 1, whereas the objective of this part is to explore in more detail the influence of the turbulence characteristics of the flow on heat transfer. In particular, the effect of naturally occurring vortices on the mean heat transfer from the impingement surface is presented.

In a jet flow, vortices initiate in the shear layer due to Kelvin Helmholtz instabilities. As the vortices move downstream of the jet nozzle each vortex can be wrapped and develop into a three dimensional structure due to secondary instabilities. These secondary instabilities can lead to the "cut and connect" process as described by Hui et al. [1] and Hussain [2] in which the toroidal vortices break down into smaller scale motions, generating high turbulence. Vortices, depending on their size and strength, affect the jet spread, the potential core length and the entrainment of ambient fluid. In certain cases jet vortices can pair, forming larger but weaker vortices. In general, vortices pass in the shear layer of the jet at the same frequency as that at which they roll up but in the vortex pairing case the passing frequency halves as the vortices pair off. Turbulent jets have a fundamental frequency at which the pairing process stabilises and this is determined by the turbulence level of the jet. With distance from the jet nozzle the vortices break down into random small scale turbulence. It is clear that vortices influence the arrival velocity of the impinging jet flow and therefore influence the shape and magnitude of the heat transfer distribution.

Artificial jet excitation can control the development of vortices in the jet flow and therefore is thought to have the potential to enhance heat transfer from the surface. Liu and Sullivan [3] excited an impinging air jet acoustically and reported on the resulting flow and heat transfer distributions. It was found that, depending on the fre-

* Corresponding author. Tel.: +353 1 896 3878; fax: +353 1 679 5554.
E-mail address: tadhg.odonovan@tcd.ie (T.S. O'Donovan).

0017-9310/$ - see front matter
doi:10.1016/j.ijheatmasstransfer.2007.01.047

Nomenclature

D	diameter (m)	U	velocity (m/s)
f	frequency (Hz)	x	distance from nozzle exit (m)
H	height of nozzle above surface (m)		
Nu	Nusselt number, hD/k (−)	*Greek symbols*	
Nu'	root-mean-square Nusselt number (−)	δ	distance between sensors (m)
r	radial distance from geometric centre (m)	μ	viscosity (kg/m s)
Re	jet Reynolds number, $\rho U D/\mu$ (−)	ρ	density (kg/m^3)
St	Strouhal number, fD/U (−)	Φ	phase (−)

quency of excitation, the area averaged heat transfer could be enhanced or reduced at low nozzle to impingement surface spacings. In the case where the jet is excited at a subharmonic of the natural frequency of the jet, the heat transfer is reduced; this frequency has the effect of strengthening the coherence of the naturally occurring frequency. The jet was also excited at a frequency higher than that of the natural jet frequency. In this case the excitation had the effect of producing intermittent vortex pairing, resulting in a break down of the naturally occurring vortices. The resulting transition to small scale turbulence effectively increases the heat transfer to the impinging air jet.

In recent times control of the jet vortex flow has attracted much research interest as the latest parameter identified as important for impinging jet heat transfer. Hui et al. [1] and Gao et al. [4] installed mechanical tabs at the nozzle exit to instigate streamwise vortical structures. These have the effect of increasing the secondary instabilities in the jet and therefore hasten the "cut and connect" process that breaks the vortices down into small scale turbulence. Hwang et al. [5] investigated the effect of acoustic excitation on a coaxial jet flow and explored the resulting effect on heat transfer. Hwang and Cho [6] continued this research for a wider range of test parameters. While the research to date has shown possible enhancement of the mean heat transfer at various excitation frequencies, much of this has been attributed to changes in the arrival velocities. The effect of the vortical flow structure on the local heat transfer has not been reported in depth.

The literature to date has shown that the heat transfer distribution over the impinging surface varies considerably with height of the jet nozzle above the surface. While abrupt increases in turbulence in the wall jet are used to explain the location and magnitude of secondary peaks in heat transfer the literature fails to provide an in depth explanation of the controlling heat transfer mechanism. The objective of this research is to understand the influence that the actual vortex flow structure, at various stages of its development, has on the convective heat transfer in the wall jet. Results are presented in the current investigation for a jet that is formed from a fully developed pipe flow impinging on a heated flat surface. Temporally simultaneous measurement and analysis of the surface heat flux and the local fluid velocity has revealed the effect that vortices have on both the mean and fluctuating heat transfer coefficient.

2. Experimental rig

The experimental rig consists primarily of a nozzle and a heated impingement surface. The flat impingement surface is instrumented with two single point heat flux sensors. Laser Doppler Anemometry is used to measure flow velocity and turbulence intensity at a point 3 mm above the heated surface, which was the closest possible given experimental constraints; this method has high spatial and temporal resolution. The experimental set-up is shown in Fig. 1. The experimental rig design and the heat transfer measurement techniques employed are described in detail in part 1 of this two part investigation.

The Laser Doppler Anemometry system is based on a Reliant 500 mW Continuous Wave laser from Laser Physics. This is a two component system and therefore the laser is split into 2 pairs of beams, that have wavelengths of 514.5 nm (green) and 488 nm (blue), to measure the velocity in orthogonal directions at the same point location. The four beams, each of diameter 1.35 mm, are focused on a point 250 mm from the laser head. The system works in backscatter mode and a base spectrum analyser (BSA) acquires and processes the signal to compute the velocity. Food grade polyfunctional alcohol liquid particles, typically 1–50 μm in diameter were used to seed both the jet flow and the ambient air.

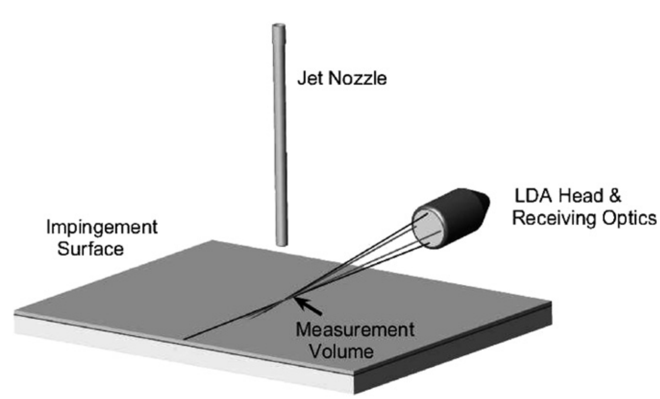

Fig. 1. Laser doppler anemometry measurement set-up.

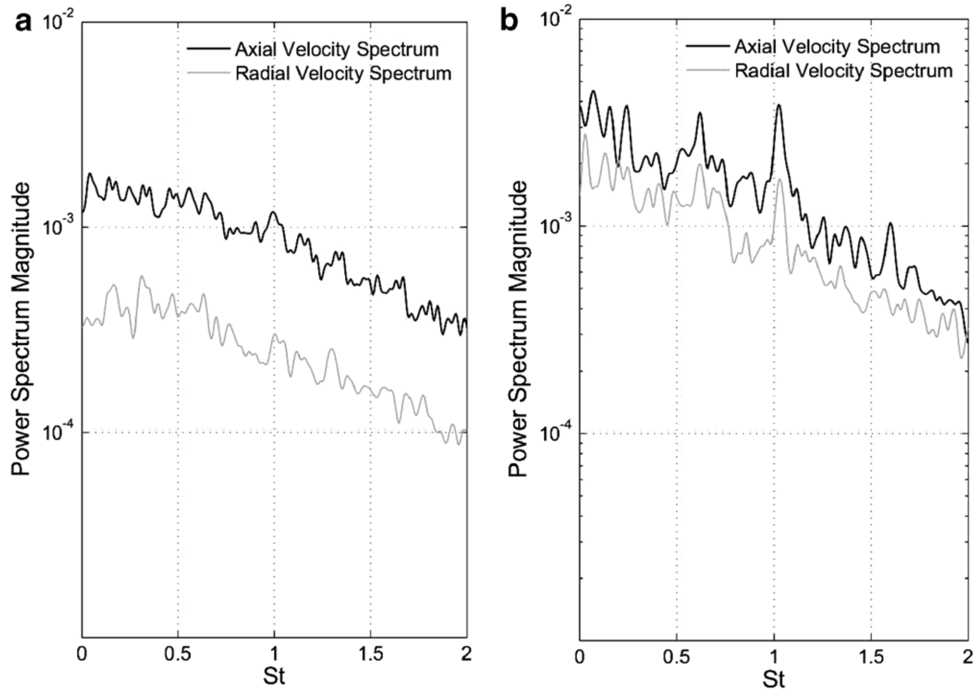

Fig. 2. Free jet velocity spectra; $x/D = 0.5$. (a) Centreline, $r/D = 0$ and (b) shear layer, $r/D = 0.35$.

The measurement of velocity is dependent on a seeding particle passing through the interrogation zone and therefore the velocity is randomly sampled at an irregular time interval. As a consequence each test point will also have different sample rates. Data presented have a minimum acquisition frequency of 8 kHz to ensure that the effect of coherent structures within the flow is measured. To process the data the signal must be re-sampled at a much higher frequency and at a regular time step. This introduces an error in the signal. There are several methods of re-sampling such as Sample and Hold, Slotting, Decimation, Spline Interpolation, etc. In this investigation the signal has been re-sampled using Sample and Hold and a correction for error is performed according to Fitzpatrick and Simon [7]. A trigger mechanism ensured the simultaneous acquisition of both fluid velocity and heat transfer signals.

3. Results and discussion

The results are presented in two sections. The first section presents fluid velocity data at the exit of a free jet. The second section presents heat transfer and local fluid velocity data at various locations in the wall jet.

3.1. Free jet fluid velocity

A Fourier transform of the velocity signals was used to calculate the velocity power spectrum which is a plot of the signal power over the frequency range. The velocity spectra at the centreline of the jet and in the shear layer are presented in Fig. 2. The frequency (f) of fluctuations is presented in the non-dimensional form of the Strouhal number, defined by:

$$St = \frac{fD}{U_{\text{jet}}} \quad (1)$$

where U_{jet} is the jet exit velocity. In both the centreline and shear layer flow the spectral power density is lower for the radial velocity component. This indicates that the velocity fluctuations are greatest in the main jet flow direction. Overall, however, the spectral power is far greater in the turbulent shear flow region. It is apparent that no dominant frequency exists in the jet centreline flow and that the velocity fluctuations reflect random small scale turbulence. In the shear layer, however, three dominant peaks in the power spectrum are evident at Strouhal numbers of approximately 0.6, 1.1 and 1.6, respectively. Schadow and Gutmark [8] reported similar frequencies that occur at the exit of their jet. The highest of the three frequencies was attributed to the frequency at which vortices roll up in the shear layer whereas lower frequencies are attributed to the frequencies at which vortices pass following merging processes. In the investigation of Han and Goldstein [9], two peaks were found in the velocity spectra. The higher frequency peak was attributed to the roll-up or passing frequency of the vortex. The lower frequency peak, however, only occurred at larger distances from the nozzle exit and was attributed to vortex pairing. In the current investigation it is thought that vortex pair-

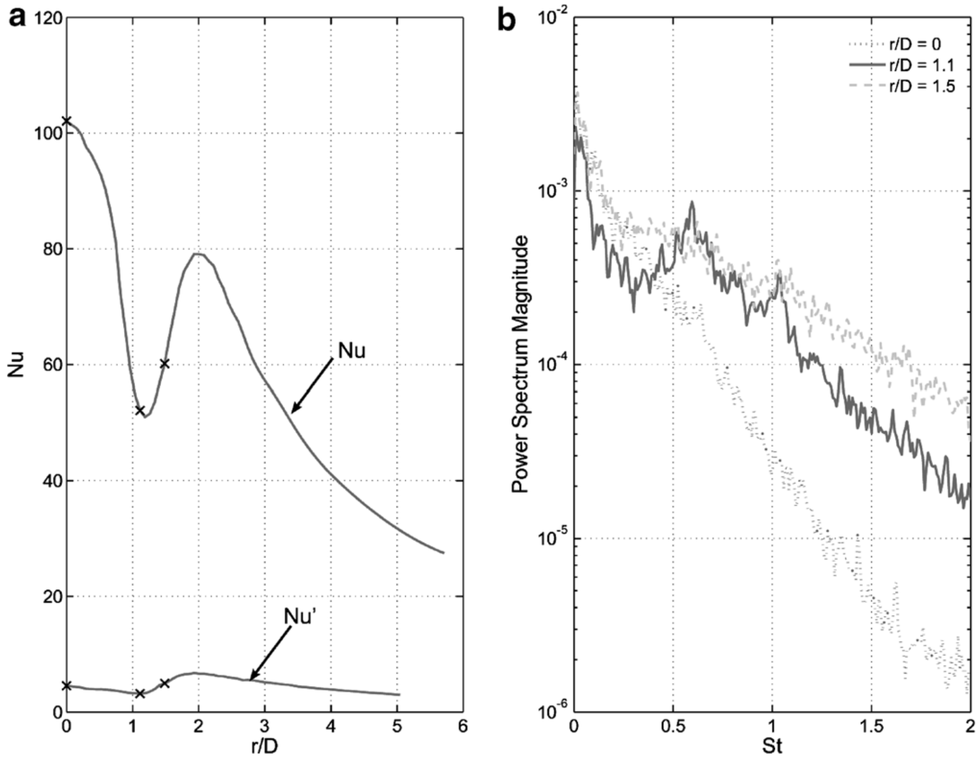

Fig. 3. *Nu* distribution and heat flux spectra; $Re = 30{,}000$, $H/D = 1.5$.

ing occurs earlier due to the relatively high turbulence at the jet exit.

3.2. Wall jet

The radial distribution of mean heat transfer for a jet impinging at low nozzle to plate spacings contains a secondary peak which is not evident for a jet impinging at a large spacing. As discussed in part 1, this secondary peak is associated with the transition to turbulence within the wall jet.

Fig. 3 presents both the mean and fluctuating Nusselt number distributions and identifies the locations in the boundary layer at which spectral analysis is performed on the heat flux signal. The spectrum at the stagnation point exhibits no dominant frequency peak and decays to a low turbulence level. At a location approaching the trough in the heat transfer distributions ($r/D = 1.1$) a dominant frequency peak occurs in the spectrum at a Strouhal number of approximately 0.6. This Strouhal number corresponds to the frequency of vortex resulting from the merging process of higher frequency vortices evident at the exit of the free jet. Beyond this radial distance, however, the vortex begins to be broken down as the wall jet flow undergoes transition to a fully turbulent flow where only small scale flow structures survive. At $r/D = 1.5$ the power dissipated at high frequencies is increased substantially relative to the shorter radial distances considered. This is a further indication that the coherent vortical flow structure is being broken down into small scale, higher frequency random turbulence.

The heat transfer spectrum has been investigated for the entire range of parameters studied. It has been found that at low H/D and at specific locations along the impingement surface there are dominant frequencies at which the heat transfer fluctuates. The frequency peaks occur in the spectrum of the heat flux signal at a radial location which depends on Reynolds number and on nozzle to impingement surface spacing. This frequency peak is most pronounced at locations approaching the trough in the mean Nusselt number distribution. The effects of the vortex are also evident at smaller radial distances but to a lesser extent, and as the structure moves along the wall jet it eventually breaks down into smaller scale turbulence. The peak in the heat transfer spectrum occurs at a higher frequency with increasing *Re*, as evident from the time trace of the Nusselt number signal presented in Fig. 4b. (Fig. 4a identifies the location on the mean heat transfer distribution to which the time trace corresponds.) It is found that the frequency of the heat transfer fluctuations is directly proportional to the jet Reynolds number, as expected.

Temporally simultaneous measurements of local fluid velocity and heat transfer were made for $H/D = 0.5$, 1.0, 1.5, 2.0; radial distance, $0 < r/D < 3$ and Reynolds number, $Re = 10{,}000$. Both the axial and radial velocity components 3 mm above the plate exhibit many of the characteristics of the surface heat transfer, although the influence of the fluctuating velocities on the heat flux varies with the location

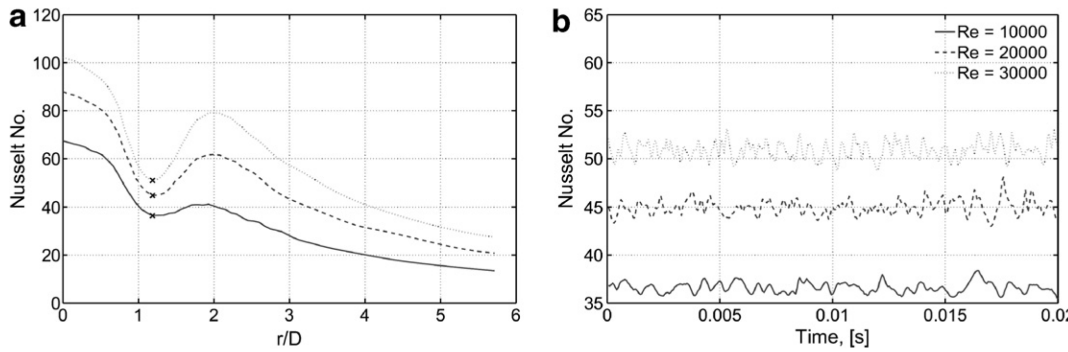

Fig. 4. Normally impinging jet; $H/D = 1.5$. (a) *Nu* distribution and (b) *Nu* time-trace.

on the impingement surface. At low H/D the dependence on radial location is very significant due to the velocity gradients involved in this particular jet set-up. It has been found that the heat transfer at the stagnation point is largely dependent on the axial velocity; this is also true for any radial location within the stagnation zone.

In Fig. 5 the locations at which temporally simultaneous measurements were made for H/D of 0.5 are marked on the velocity and heat transfer distributions. The local fluid velocity signals in both the axial and radial directions have been cross correlated with the heat flux signal to calculate the coherence (similarity) and phase difference between the signals. The coherence between the heat flux and the velocity perpendicular to the surface (axial velocity) is shown in Fig. 6 to be significant at $0.37D$ from the stagnation point, decreasing from a value of 0.5 with increasing frequency. From the phase difference between the axial velocity and the heat flux signals, the convection velocity (U_c) normal to the impingement surface can be calculated as indicated in Eq. (2).

$$U_c = \frac{2\pi\delta f}{\Phi}, \tag{2}$$

where δ is the distance between the velocity and heat flux measurement points, f is the frequency at which the convection velocity is calculated and Φ is the phase difference between the two signals. The convection velocity in this case is approximately 9.8 m/s. At this location, the coherence between the heat flux and the radial velocity is less than 0.1 and consequently the phase difference between the two signals is of no significance. The dependence of the heat flux on the axial velocity fluctuations is consistent with the axial fluctuations being greater in magnitude than those parallel to the surface.

At the greater radial distance of $r/D = 0.65$, presented in Fig. 7, the Strouhal number of 1.6 corresponds to the frequency at which vortices roll up at the jet exit while the lower Strouhal number of 1.1 relates to passing frequency of a larger vortex that has developed following a merging process. The velocity spectra indicate that the two frequency peaks have quite similar magnitudes suggesting that the vortex merging process is in progress. The heat flux spectrum is clearly influenced by both velocity signals. The coherence between the heat flux and both axial and radial velocities is higher at this larger radial distance, particularly in the frequency range associated with the coherent flow structure that impinges upon the surface at this location. While the radial velocity component has more of an influence on the heat flux at this radial location than in the stagnation zone, the higher coherence values suggest that the axial velocity remains the main influence on surface heat flux. With regard to the phase difference, the convection velocity has increased, with the greater radial distance, to approximately 13.5 m/s. The coherence between the radial

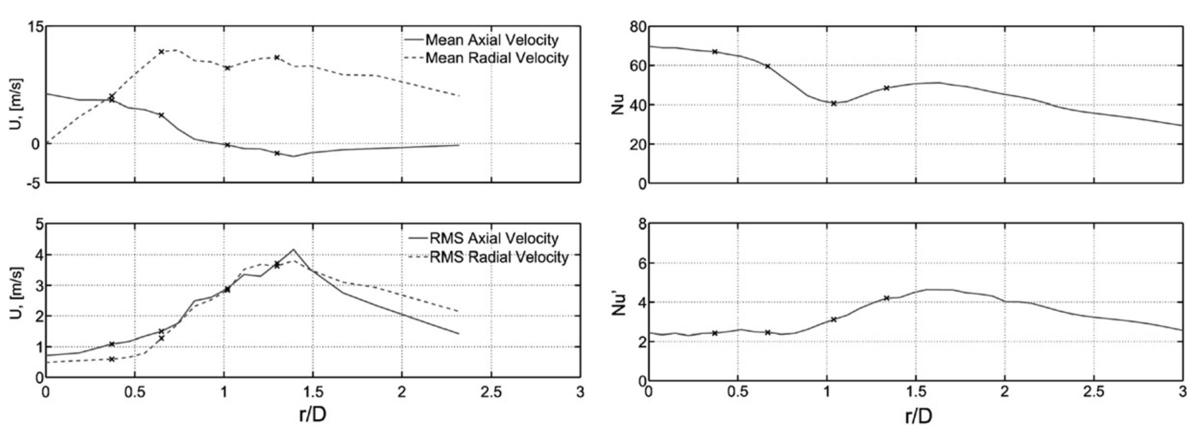

Fig. 5. Radial location of simultaneous measurements; $H/D = 0.5$.

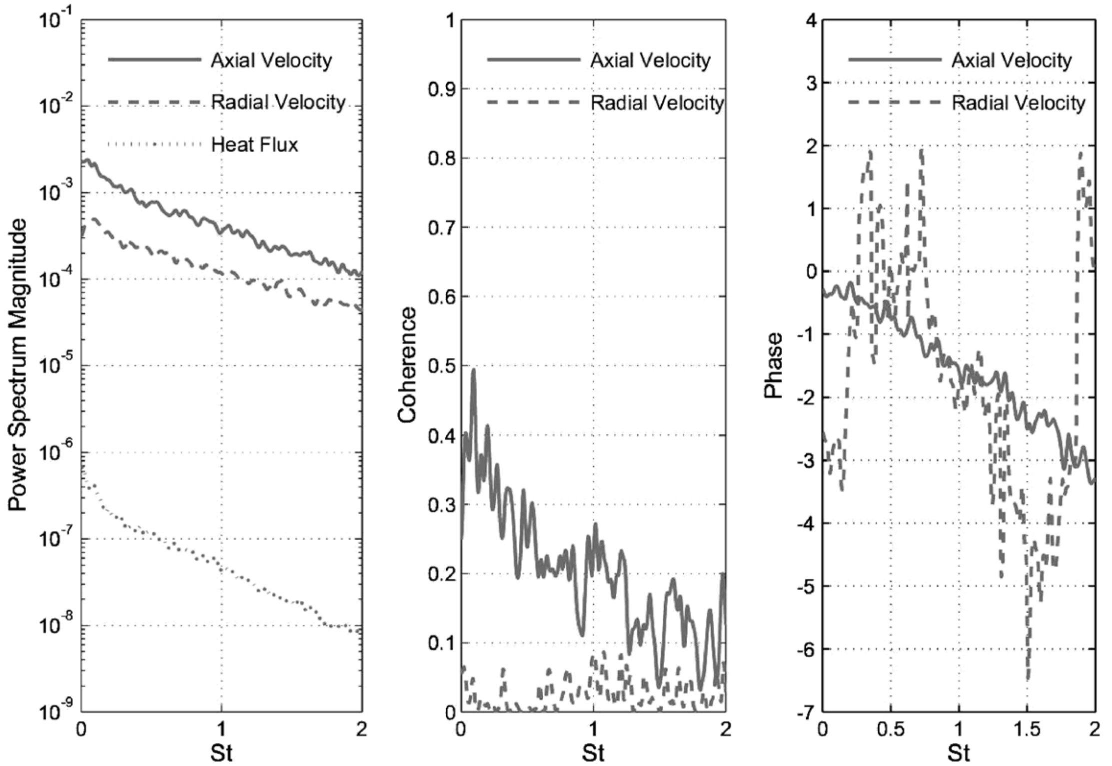

Fig. 6. Power spectra and coherence and phase information between velocity and heat flux signals; $H/D = 0.5$, $r/D = 0.37$.

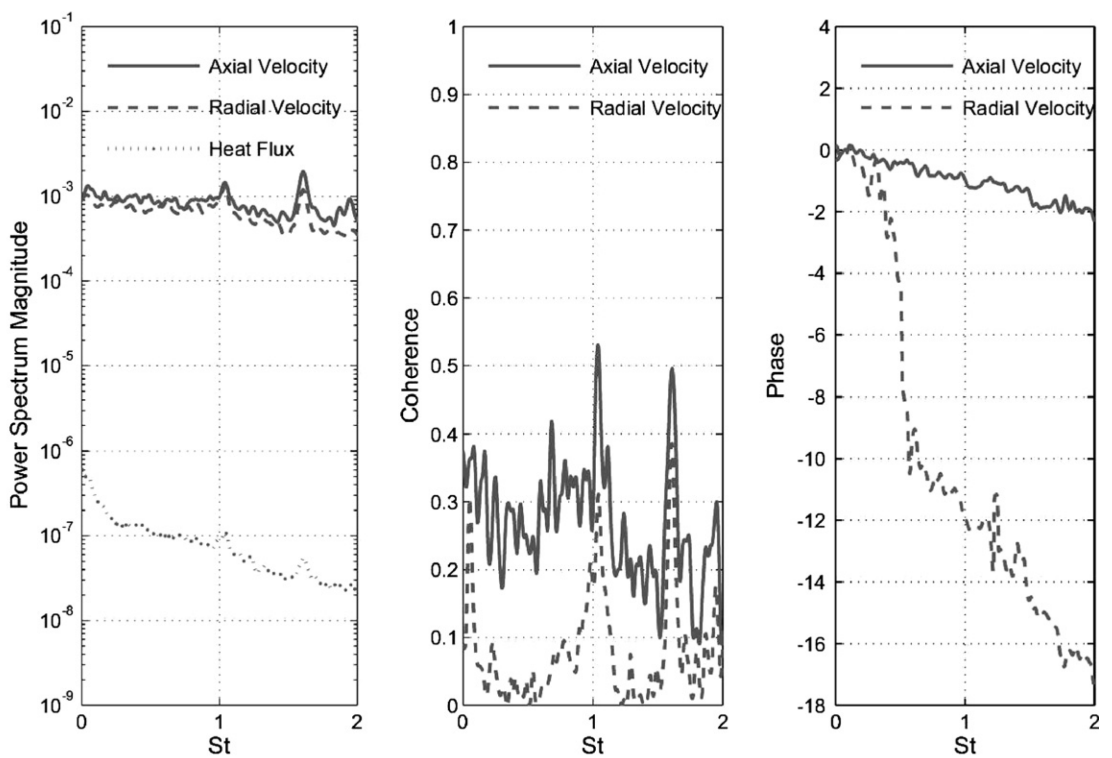

Fig. 7. Power spectra and coherence and phase information between velocity and heat flux signals; $H/D = 0.5$, $r/D = 0.65$.

velocity and the heat flux signal is sufficient to get good phase information in the middle frequency range. However, the slope of the phase difference between the radial velocity and heat flux signals is very different to that between the axial velocity and the heat flux at this radial location. Effectively the radial convection velocity is much lower than the axial convection velocity. The difference can be attributed to the location of the heat flux measurement point with respect to the velocity component being measured. The axial convection velocity is in line with the axial flow velocity and fluctuations in the flow in this direction convect directly towards the heat flux sensor. The radial convection velocity is measured perpendicular to the direction of the radial velocity. Therefore fluctuations in the radial direction convect at a lower rate towards the heat flux sensor. Consequently the radial convection velocity is lower than the axial convection velocity throughout the range of tests presented.

Temporally simultaneous velocity and heat flux measurements at even greater radial locations for $H/D = 0.5$ are presented in Figs. 8 and 9. At these larger distances from the geometric centre the lower Strouhal number of 1.1 exhibits the slightly larger peak in the velocity and heat flux spectra. This indicates that vortices continue to merge within the wall jet. The radial velocity spectrum indicates that the vortex merging process is at a more advanced stage than the axial velocity suggests. One possible explanation for this is given by the findings of Orlandi and Verzicco [10] who investigated vortex rings impinging on a wall. In this computational investigation it has been shown that merging vortices present as one large vortex in the radial direction, while remaining separate entities in the axial direction. At the location of $r/D = 1.02$ the coherence between the velocity signals and the heat flux is greater than for any other radial location investigated. Again the axial velocity has slightly higher coherence with the heat flux than the radial velocity, even though the magnitude of the fluctuations in both the axial and radial directions is similar, as shown in Fig. 5. This is understandable as temperature gradients normal to the surface are greater than parallel to the surface. Beyond this radial distance the peaks in all spectra reduce in size as can be seen at $r/D = 1.30$. In this region the turbulence in the wall jet increases, breaking the coherent vortex down into random small scale velocity fluctuations. The phase information indicates that the convection velocity in the axial direction has decreased once again and this is most likely due to the decreased mean velocity in this direction. The axial convection velocities are calculated to be 18.7 m/s and 7.3 m/s for $r/D = 1.02$ and 1.30, respectively.

A similar analysis of temporally simultaneous velocity and heat flux measurements has been conducted for a jet impinging at nozzle to plate spacings of $H/D = 1.0$, 1.5 and 2.0. For these spacings, spectral, coherence and phase information for the velocity and heat flux signals are presented in Figs. 10–12 at $r/D = 1.02$, as this is where vortices within the flow are most coherent.

It can be seen in Fig. 10 that the dominant frequency peaks occur at Strouhal numbers of 0.6 and 1.1 at $H/D = 1$. Also, a slight peak is evident at $St = 1.6$. It is apparent that the vortices which rolled up at the jet nozzle have merged to form larger vortices at a lower frequency. This new vortex is also undergoing a second merging process and this results in a peak at the low Strouhal number of 0.6. The radial velocity spectrum indicates that the two frequency peaks have similar magnitudes, suggesting that the

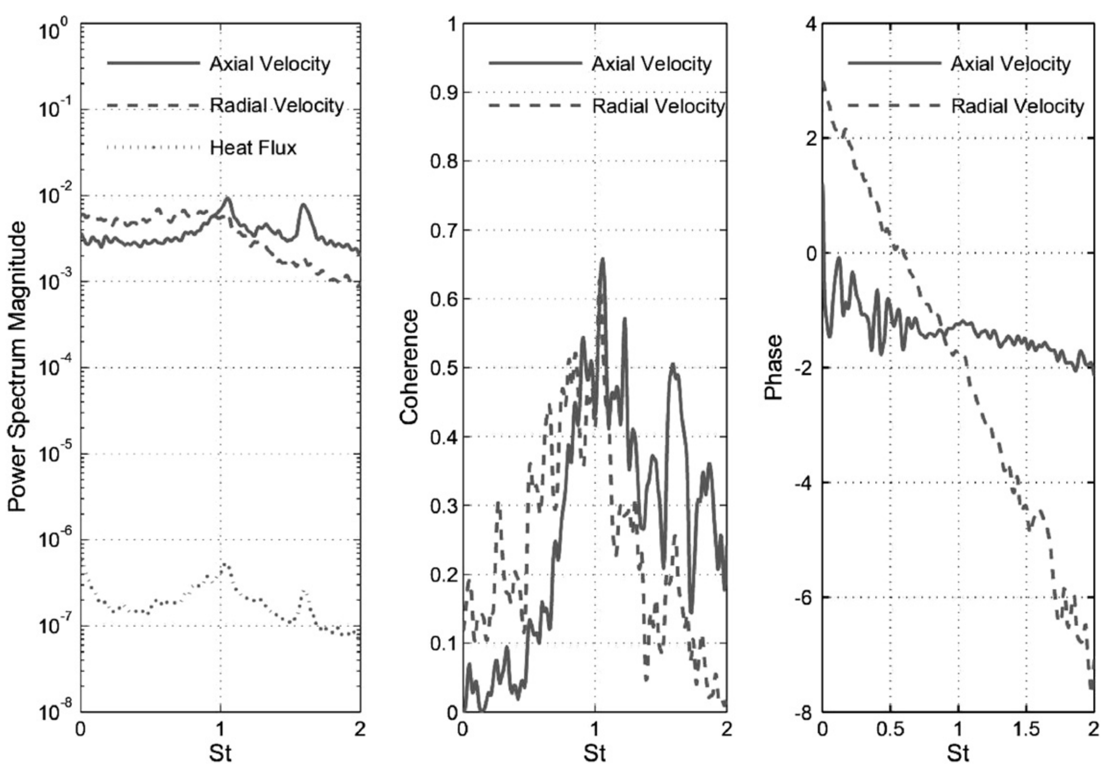

Fig. 8. Power spectra and coherence and phase information between velocity and heat flux signals; $H/D = 0.5$, $r/D = 1.02$.

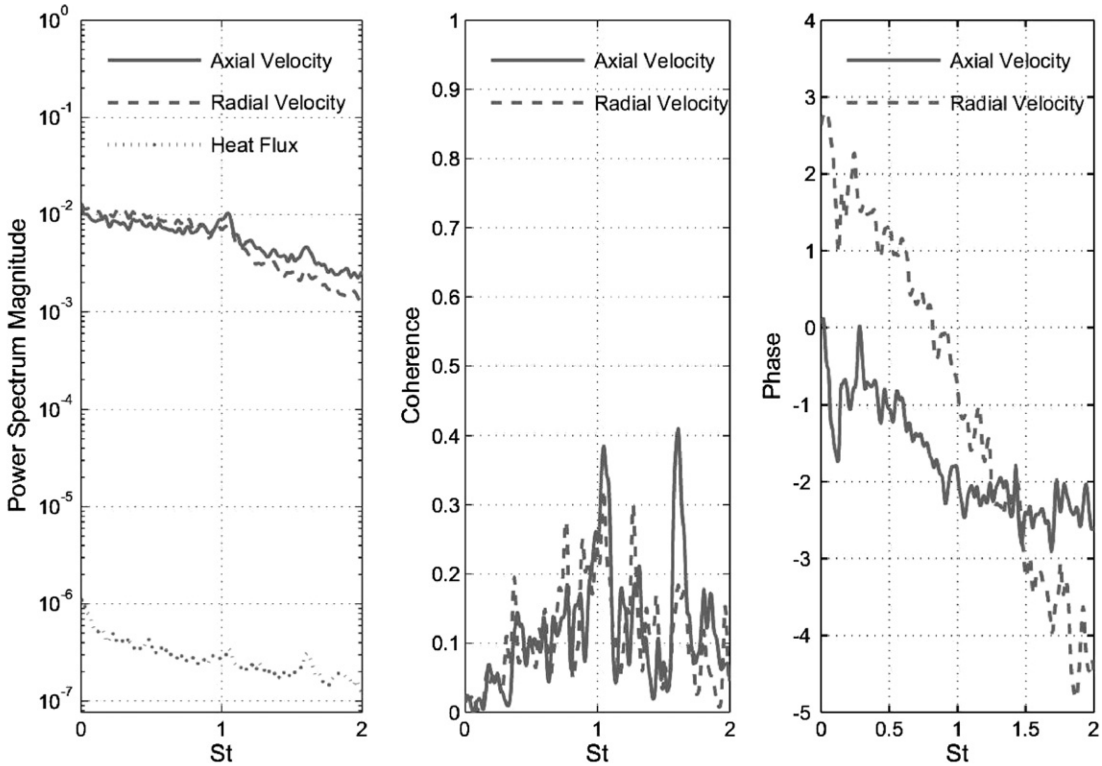

Fig. 9. Power spectra and coherence and phase information between velocity and heat flux signals; $H/D = 0.5$, $r/D = 1.30$.

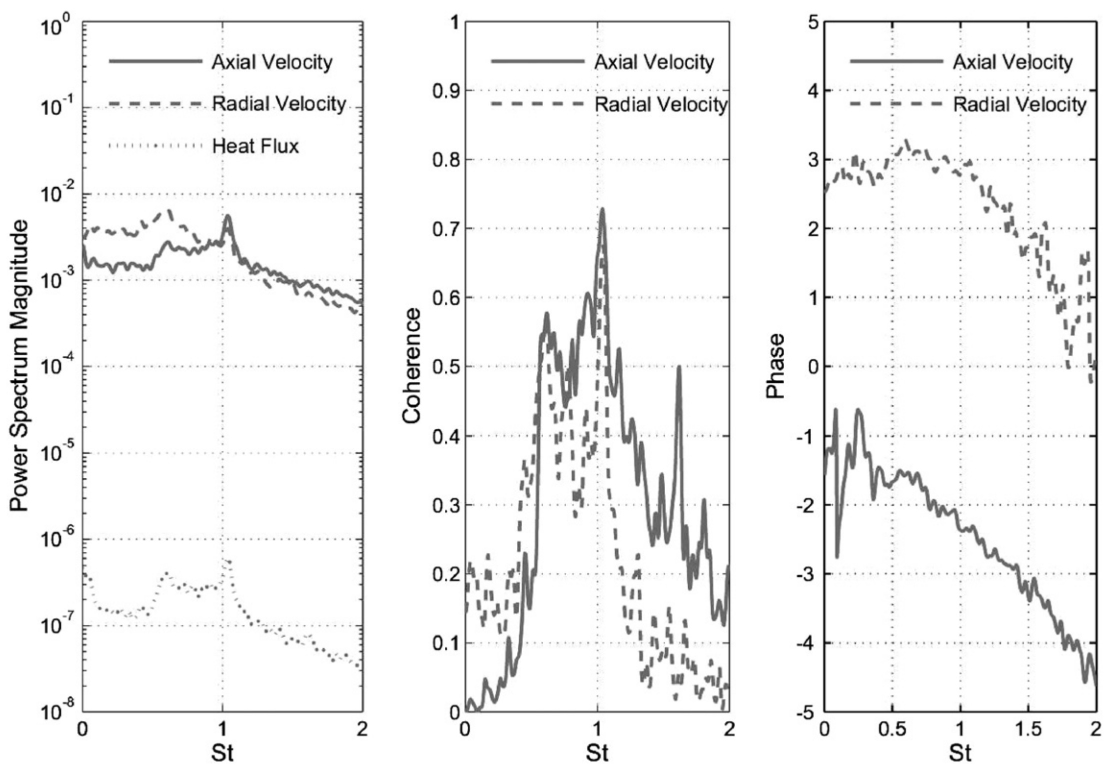

Fig. 10. Power spectra and coherence and phase information between velocity and heat flux signals; $H/D = 1$, $r/D = 1.02$.

second vortex merging process is in progress. The axial velocity spectrum, however, shows the peak at the higher frequency to have the greater magnitude, suggesting that this second vortex merging is in its initial stages.

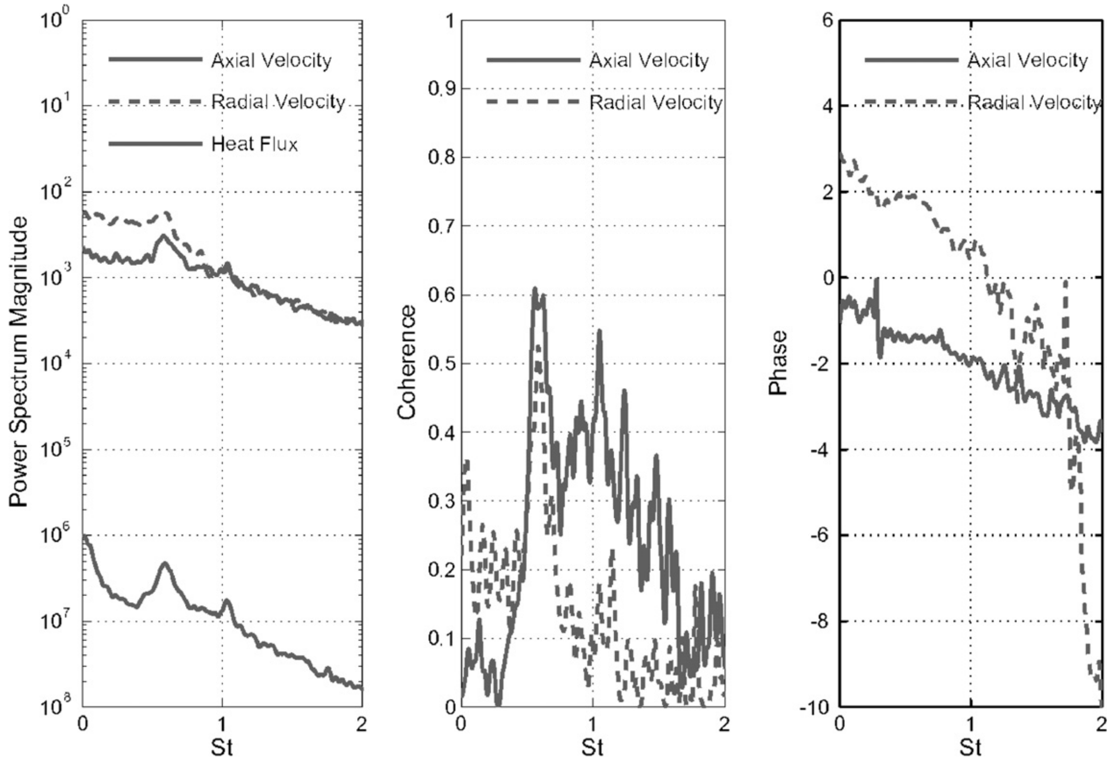

Fig. 11. Power spectra and coherence and phase information between velocity and heat flux signals; $H/D = 1.5$, $r/D = 1.02$.

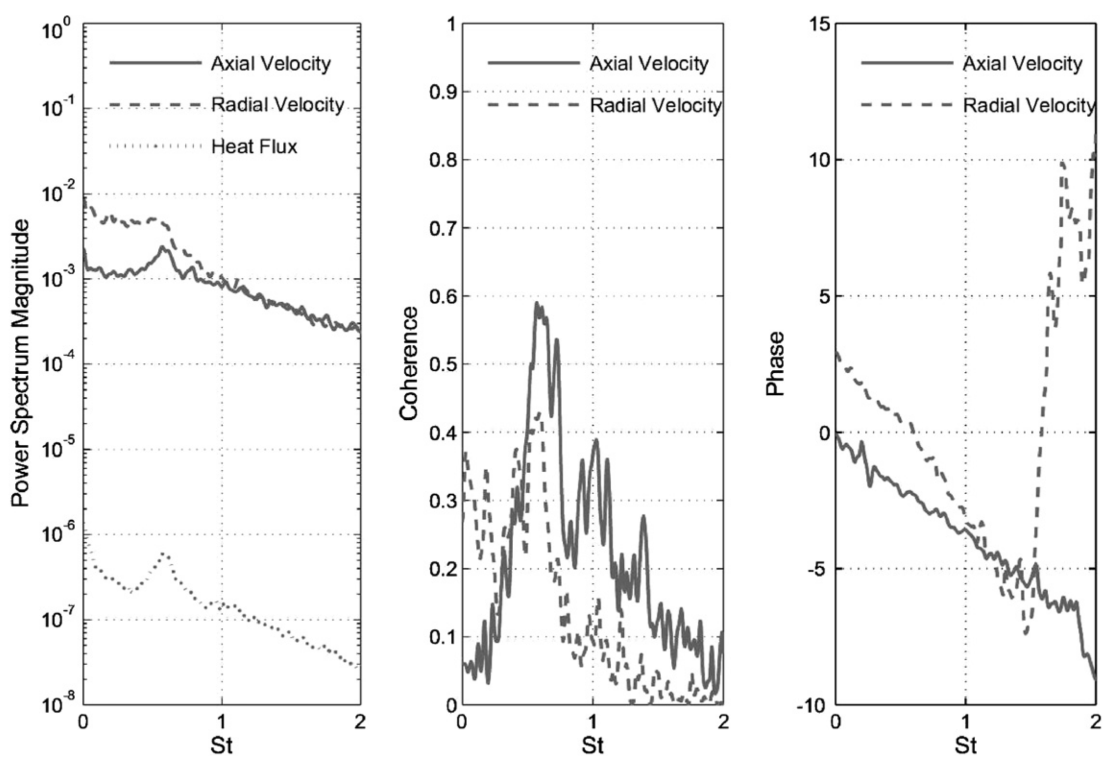

Fig. 12. Power spectra and coherence and phase information between velocity and heat flux signals; $H/D = 2$, $r/D = 1.02$.

At $H/D = 1.5$ (Fig. 11) the vortices have grown in size due to the vortex merging process. Two dominant peaks are evident in the individual spectra at $St = 0.6$ and 1.1. In general the two peaks have similar magnitudes indicating that the second vortex merging process is in progress. Once again, the spectrum of the radial velocity indicates that the vortex merging process is further advanced as the peak at the lower Strouhal number of 0.6 has the greater magnitude. Also, the coherence between the radial velocity and the heat flux is low at the higher Strouhal number ($St = 1.1$). Once again the influence on heat transfer of velocity fluctuations normal to the impingement surface is shown to be more significant.

Finally, at $H/D = 2$ only one dominant peak remains in all three spectra, at a Strouhal number of 0.6. The vortex that passes at this frequency was evident across the range of radial locations tested, but was found to be most coherent at $r/D = 1.02$, as the case shown in Fig. 12. At this stage it is apparent that the second merging process has completed to form one large vortex that passes at a Strouhal number of approximately $St = 0.6$. According to Broze and Hussain [11], this Strouhal number is consistent with the natural frequency that is expected for a jet that issues with a turbulence level of approximately 30%.

In general, for a normally impinging jet with $H/D \leqslant 2$ the heat flux exhibits a significant dependence on velocity fluctuations normal to the impingement surface. Even in cases where velocity fluctuations parallel to the surface are greater than normal to the surface, the heat transfer relies substantially on the axial fluctuations. The variation

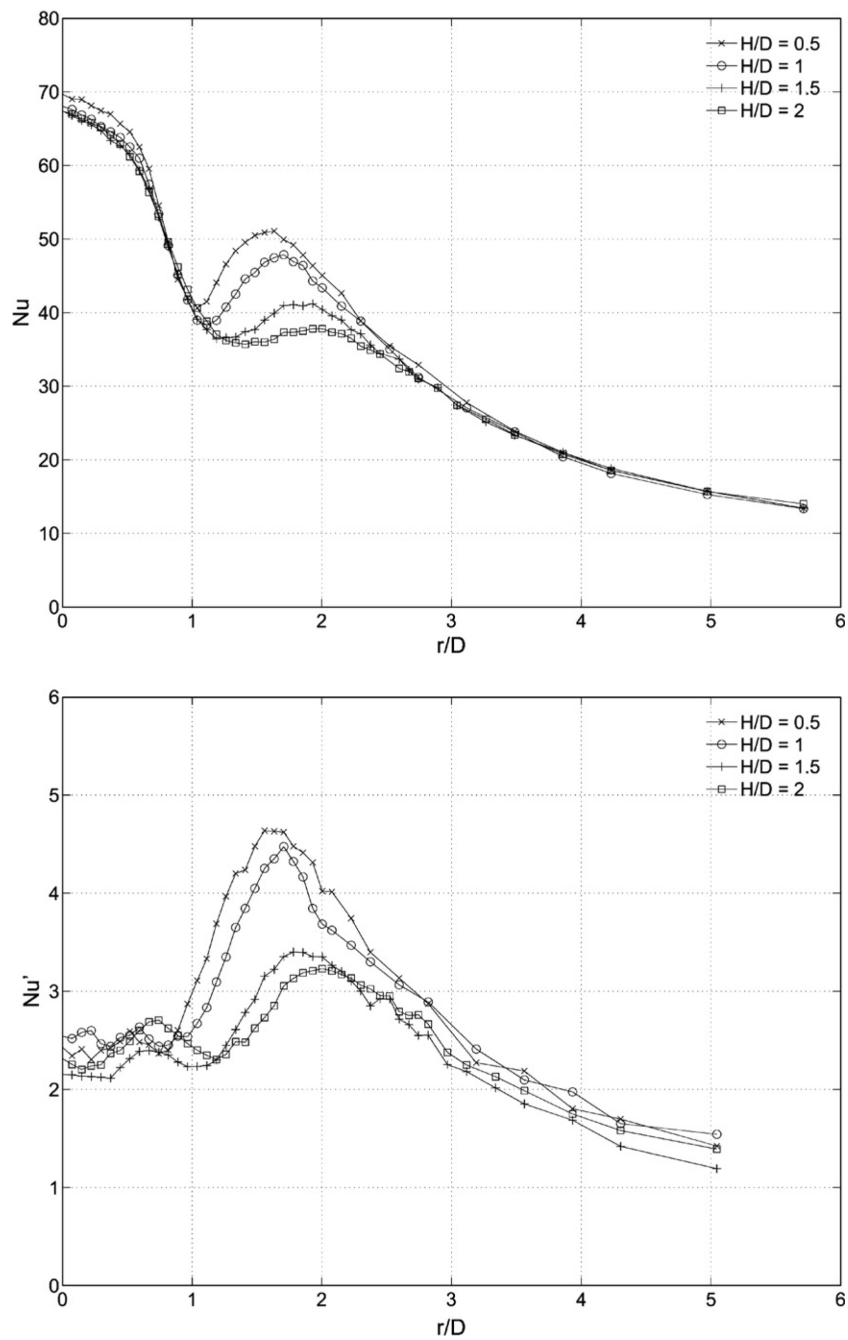

Fig. 13. Mean and fluctuation nusselt number distributions; $Re = 10{,}000$.

of H/D from 0.5 to 2 has seen vortices at different stages of their development impinge upon the heated surface. At $H/D = 0.5$ the vortices are strong and initiate and pass at high frequencies. At larger H/D the vortices merge, and pass along the wall jet at lower and lower frequencies.

By reviewing the mean velocity and heat transfer distributions (discussed in more detail in part 1) at different stages within the vortex development, a fuller understanding of the influence of the vortices can be achieved. Fig. 13 presents the mean heat transfer distributions at low nozzle to impingement surface spacings. It is apparent that both the mean and fluctuating Nusselt number distributions converge in the stagnation zone ($r/D < 1$) and in the fully developed wall jet region ($r/D > 2.5$). Fig. 14 presents the mean velocity distributions for the four different heights. There is no significant difference between the radial velocity distributions, however a slight trend with H/D can be appreciated for the mean axial velocity distributions. At H/D of 0.5, at the first stage of the vortex development, the axial velocity is more negative at around $1 < r/D < 1.5$ which corresponds to the vortex impinging on the wall jet. It has been shown, by Didden and Ho [12], that strong vortices in the wall jet have the effect of inducing flow separation; the axial velocity distributions reported here are

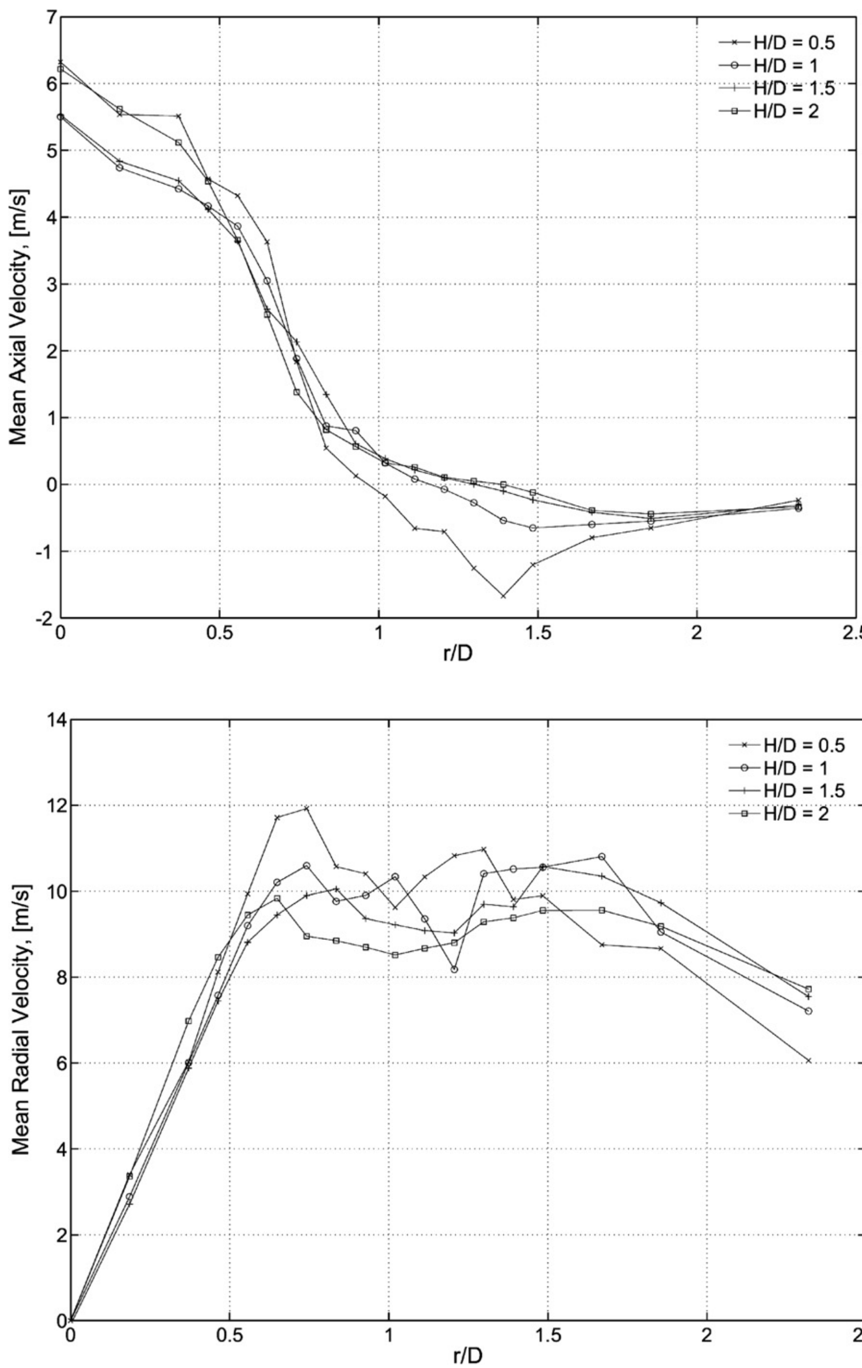

Fig. 14. Mean velocity distributions; $Re = 10{,}000$.

consistent with this. Otherwise the axial velocity distributions coalesce in the same location as the Nusselt number distributions. Finally the distributions of the rms velocity are presented in Fig. 15. The magnitude of the fluctuations in the radial velocity has been influenced slightly by the various stages of the vortex development. It has been shown to date that fluctuations in the radial direction have less of an influence on the heat transfer than the fluctuation normal to the impingement surface. At the different nozzle heights above the impingement surface the velocity fluctuations normal to the impingement surface have changed significantly. Since the mean velocity distributions are relatively unchanged the variation in the velocity fluctuations is attributed to the variation in the vortical nature of the impinging jet flow.

Although vortices delay the transition to a fully turbulent flow in the wall jet, the eventual breakup of vortices induces velocity fluctuations normal to the impingement surface that increase surface heat transfer. In general, when a vortex impinges at the early stage of its development, it is strong and maintains the low turbulence in the wall jet. Breakup of this strong vortex, however, results in large axial velocity fluctuations that enhance the mean surface heat transfer. When the vortex impinges on the surface at

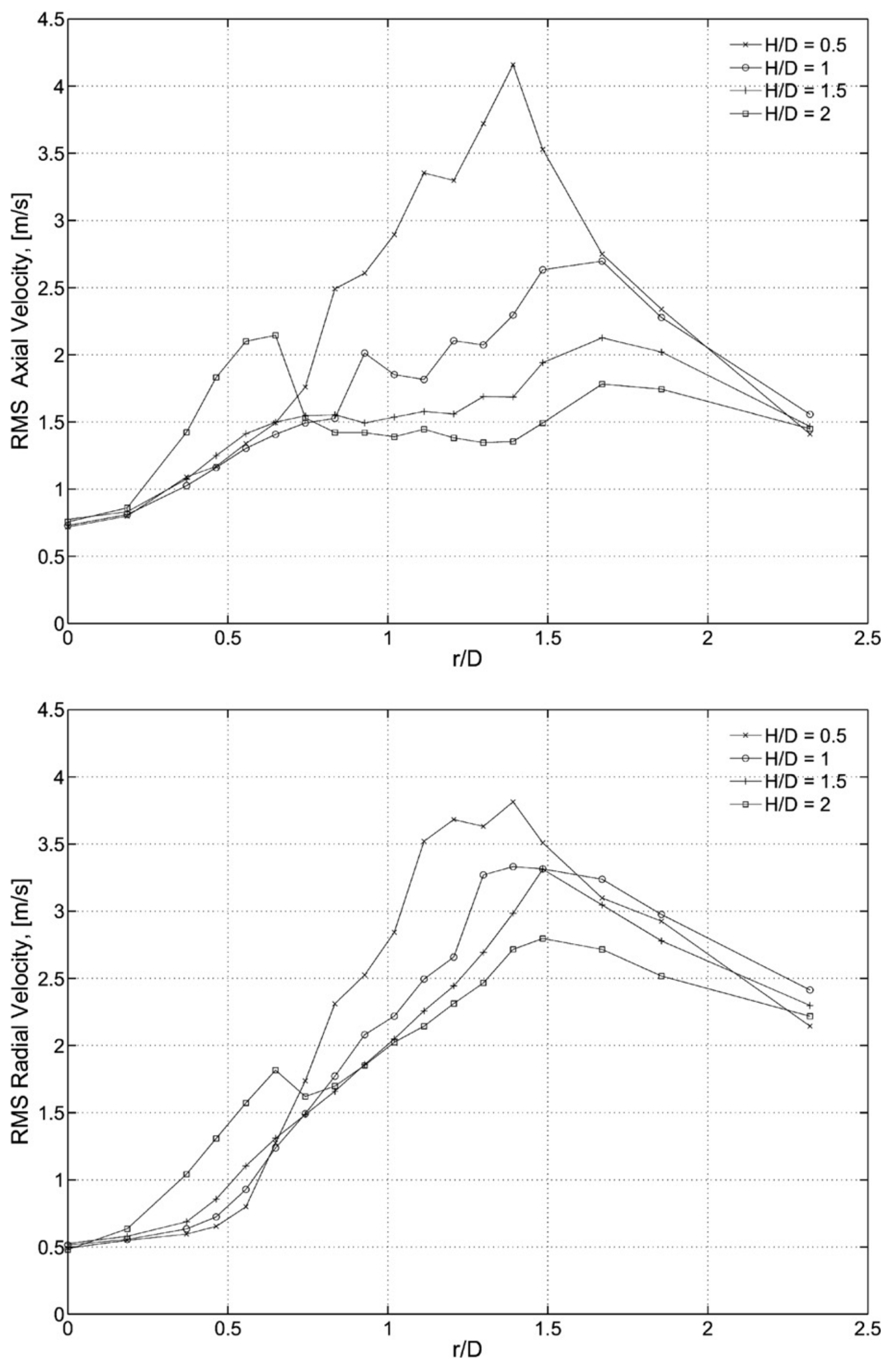

Fig. 15. RMS velocity distributions; $Re = 10{,}000$.

later stages of its development, its effects are less pronounced. The breakup of this weaker vortex results in lower magnitude axial velocity fluctuations and therefore does not increase the surface heat transfer to the same extent.

At large H/D (>2) secondary peaks in the mean heat transfer profile may still exist, however no dominant frequency was found in the heat transfer spectrum for jet to plate spacings from $2D$ to $8D$. For this reason the results presented here have been limited to the low range of $H/D \leqslant 2$.

4. Conclusions

Results presented in part 1 of this investigation have shown that regions of high heat transfer are associated with regions of high local fluid velocity and turbulence intensity. In particular, peaks in the heat transfer distributions have been shown to coincide with locations where velocity fluctuations normal to the impingement surface are large. Comparison of the velocity flow fields with heat transfer distributions revealed local areas for which time-resolved data are needed.

The effect that the actual vortex structure has on surface heat transfer has attracted little attention to date. Vortices that roll-up naturally in the shear layer of the free jet, close to the nozzle exit, have been shown to merge forming larger yet weaker vortices, before being broken down into smaller scale random turbulence. Stages within the merging processes have been identified to occur at various distances from the jet nozzle. Upon impingement the vortices move along the wall jet before being broken down. The coherence of the vortical structures has the effect of maintaining the relatively low turbulence in the wall jet flow. These vortices eventually do break down and the turbulence level within the wall jet increases significantly, which in turn increases the heat transfer, leading to a secondary peak in the heat transfer distribution.

Initially, the temporal nature of the velocity at the exit of the free jet was investigated. This revealed three frequency peaks which have been associated with the roll-up and merging frequency of the vortices in the shear layer. At $H/D < 2$ similar peaks have been observed in the spectra of the heat transfer and local velocity signals in the transitional wall jet region. Temporally simultaneous local velocity and heat flux measurements have revealed that axial velocity fluctuations exhibit higher coherence with the heat transfer signal. As the height of the nozzle above the impingement surface changes from 0.5 to 2 diameters, the mean velocity in the axial and radial direction does not change significantly; the velocity fluctuations in the transitional wall jet decrease substantially however. The main difference between these heights is the stage of the vortex development. In particular, the velocity fluctuations normal to the impingement surface in the transitional wall jet have been shown to decrease substantially in the latter stages of the vortex development, leading to a reduction in the heat transfer at this location.

It has been shown here that axial velocity fluctuations close to the impingement surface have a far greater influence on the heat transfer than fluctuations parallel to the surface. Vortices that impinge upon the surface determine the magnitude and frequency of the fluctuations in both directions. Because of this, the various stages of the vortex merging process influence the mean and rms Nusselt number distributions at low H/D. When the vortices impinge upon the surface at an early stage in their development, this promotes separation in the wall jet flow and the subsequent breakup of these strong vortices leads to large velocity fluctuations normal to the impingement surface. Vortices that impinge at later stages in their development are weaker and therefore induce smaller velocity fluctuations normal to the surface as they break up. This does not enhance the heat transfer in the wall jet to the same degree as stronger vortices do. In general, the breakdown of strong vortices (in the early stages of the vortex development), has a favourable effect on the heat transfer in the near wall jet.

Acknowledgement

This work was supported in part by Enterprise Ireland under grant SC/2001/0071 and also by Science Foundation Ireland grant 04/BR/EO108.

References

[1] H. Hui, T. Kobayashi, S. Wu, G. Shen, Changes to the vortical and turbulent structure of jet flows due to mechanical tabs, Proc. Inst. Mechan. Eng. 213 (1999) 321–329.
[2] A.K.M.F. Hussain, Coherent structures and turbulence, J. Fluid Mechan. 173 (1986) 303–356.
[3] T. Liu, J.P. Sullivan, Heat transfer and flow structures in an excited circular impinging jet, Int. J. Heat Mass Transfer 39 (1996) 3695–3706.
[4] N. Gao, H. Sun, D. Ewing, Heat transfer to impinging round jets with triangular tabs, Int. J. Heat Mass Transfer 46 (2003) 2557–2569.
[5] S.D. Hwang, C.H. Lee, H.H. Cho, Heat transfer and flow structures in axisymmetric impinging jet controlled by vortex pairing, Int. J. Heat Fluid Flow 22 (2001) 293–300.
[6] S.D. Hwang, H.H. Cho, Effects of acoustic excitation positions on heat transfer and flow in axisymmetric impinging jet: main jet excitation and shear layer excitation, Int. J. Heat Fluid Flow 24 (2003) 199–209.
[7] J. Fitzpatrick, L. Simon, Estimation of cross-power spectra using sample-and-hold reconstruction of laser doppler anemometry data, Experiments in Fluids 39 (2005) 954–965.
[8] K.C. Schadow, E. Gutmark, Combustion instability related to vortex shedding in dump combustors and their passive control, Prog. Energ. Combust. Sci. 18 (1992) 117–132.
[9] B. Han, R.J. Goldstein, Instantaneous energy separation in a free jet. Part I. flow measurement and visualization, Int. J. Heat Mass Transfer 46 (2003) 3975–3981.
[10] P. Orlandi, R. Verzicco, Vortex rings impinging on walls: axisymmetric and three-dimensional simulations, J. Fluid Mechan. 256 (1993) 615–646.
[11] G. Broze, F. Hussain, Nonlinear dynamics of forced transitional jets: periodic and chaotic attractors, J. Fluid Mechan. 263 (1994) 93–132.
[12] N. Didden, C.M. Ho, Unsteady separation in a boundary layer produced by an impinging jet, J. Fluid Mechan. 160 (1985) 235–256.